Bipartite and Series-Parallel Graphs Without Planar Lombardi Drawings

David Eppstein

Department of Computer Science, University of California, Irvine

Abstract. We find a family of planar bipartite graphs all of whose Lombardi drawings (drawings with circular arcs for edges, meeting at equal angles at the vertices) are nonplanar. We also find families of embedded series-parallel graphs and apex-trees (graphs formed by adding one vertex to a tree) for which there is no planar Lombardi drawing consistent with the given embedding.

1 Introduction

Lombardi drawing is a style of graph drawing using curved edges. In this style, each edge must be drawn as a circular arc, and consecutive edges around each vertex must meet at equal angles. Many classes of graphs are known to have such drawings, including regular bipartite graphs and all 2-degenerate graphs (graphs that can be reduced to the empty graph by repeatedly removing vertices of degree at most two) [6]. This drawing style can significantly reduce the area usage of tree drawings [7], and display many of the symmetries of more general graphs [6].

Lombardi drawings have simple edge shapes and optimal angular resolution, and it is desirable to find drawings of this type that also avoid edge crossings; all of these properties lead to more readable drawings. The graphs with planar Lombardi drawings include the Halin graphs [6], 3-regular planar graphs [8], 4-regular polyhedral graphs [10], and outerpaths [5]. However, some other classes of planar graphs do not always have planar Lombardi drawings, including the nested triangle graphs [6], 4-regular planar graphs [8], planar 3-trees [5], and the graphs of knot and link diagrams [10].

For several other important classes of planar graphs, the existence of a planar Lombardi drawing has remained open. These include the outerplanar graphs, the series-parallel graphs, and the planar bipartite graphs. Outerplanar and series-parallel graphs are 2-degenerate, and always have

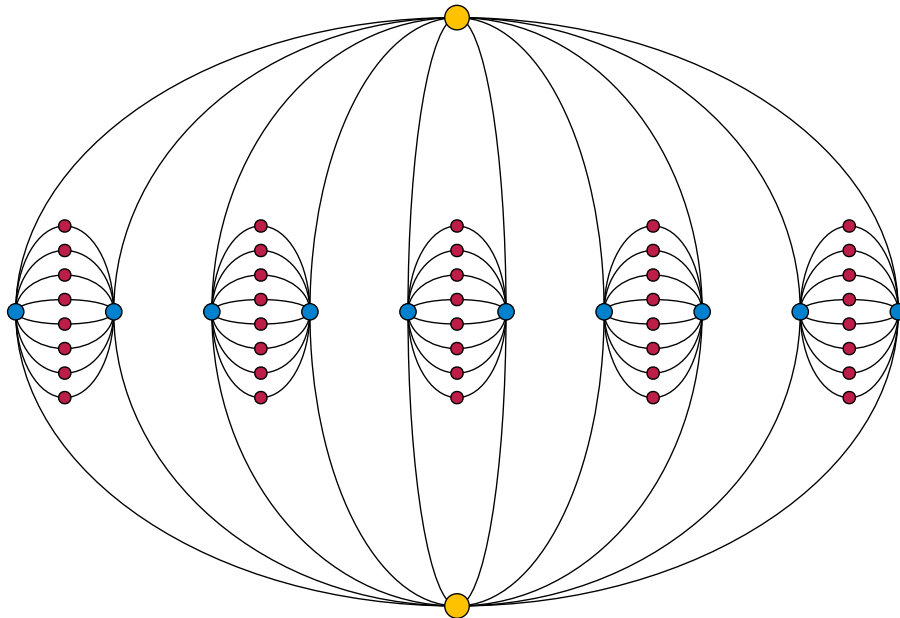*E-mail address:* eppstein@uci.edu (David Eppstein)

Figure 1: The bipartite graph $B(5)$ formed by our construction. Although drawn planarly with curved edges, this is not a Lombardi drawing: the edges are arcs of ellipses rather than of circles, and pairs of consecutive edges at the same vertex do not all have the same angles.

Lombardi drawings. Planar bipartite graphs are 3-degenerate and often have Lombardi drawings; the only obstacle to Lombardi drawing for 3-degenerate graphs is the forced placement of two vertices on the same point, but the only examples for which this is known to happen are neither planar nor bipartite [6]. However the known Lombardi drawings for these graphs are not necessarily planar. In this paper we settle this open problem for two of these classes of graphs, the planar bipartite graphs and the (embedded) series-parallel graphs. We construct a family of planar bipartite graphs whose Lombardi drawings are all nonplanar. We also construct a family of series-parallel graphs with a given embedding such that no planar Lombardi drawing respects that embedding. Our construction for series-parallel graphs can be extended to maximal series-parallel graphs, to bipartite series-parallel graphs and to apex-trees, the graphs formed by adding a single vertex to a tree.

2   The graphs

We begin by describing a family of planar bipartite graphs $B(k)$ which, for sufficiently large k, do not have planar Lombardi drawings.

Definition 1 *We define $B(k)$ to be the graph constructed as follows. Begin with a complete bipartite graph $K_{2,2k}$ and its unique planar embedding; in Fig. 1, the two-vertex side of the bipartition of this graph is shown by the yellow vertices and the $2k$-vertex side is shown by the blue vertices. Next, partition the blue vertices into k pairs of vertices, each sharing a face. For each pair of blue vertices*

in this partition, add another complete bipartite graph $K_{2,2k-2}$ connecting these two blue vertices to $2k-2$ additional vertices (shown as red in the figure).

The resulting graphs $B(k)$ are all planar, because they are formed by attaching together planar subgraphs (complete bipartite graphs where one side has two vertices) on pairs of vertices that are cofacial in both subgraphs. They are bipartite, with the yellow and red vertices on one side of their bipartition and the blue vertices on the other side. In $B(k)$, each yellow vertex has exactly $2k$ blue neighbors. Each blue vertex has exactly $2k$ neighbors, two of them yellow and the rest red. Each red vertex has exactly two neighbors. There are two yellow vertices, $2k$ blue vertices, and $k(2k-2)$ red vertices, for a total of $2k^2+2$ vertices in the overall graph. Each vertex in $B(k)$ has degree either 2 or $2k$.

These graphs are not 3-vertex-connected and (unlike the 3-vertex-connected planar graphs) have multiple non-isomorphic embeddings when viewed as labeled graphs. However Lemma 1 below demonstrates that, as unlabeled graphs, all of their planar embeddings are isomorphic. This fact will simplify our proof that they have no planar Lombardi drawing, by allowing us to consider only this unique unlabeled embedding.

Lemma 1 *Up to the choice of the outer face, all planar embeddings of $B(k)$ are topologically equivalent.*

Proof: The induced subgraph of yellow and blue vertices of $B(k)$ is a subdivision of a dipole graph (a multigraph with two vertices connected by $2k$ edges), whose embedding is unique up to permutation of its edges. In terms of $B(k)$, this means that the only way to embed this induced subgraph is to arrange the yellow-blue paths in an arbitrary cyclic order around one yellow vertex and in the opposite cyclic order around the other yellow vertex. In order for pairs of blue vertices in $B(k)$ to be connected by paths through red vertices, those blue vertices need to belong to a common face of the embedding of the dipole graph, meaning that the two paths they belong to must be adjacent in the two cyclic orderings at the yellow vertex. With this constraint, the subset of faces of the yellow-blue induced subgraph that are subdivided must form an alternating subset of the cyclic ordering of faces around each yellow vertex. Each red-blue induced subgraph is again a subdivision of a dipole, with only one planar embedding as an unlabeled graph, so each subdivided yellow-blue face must be subdivided in the same way. This completely describes the embedding, up to the choice of which face of the resulting embedding is to be the outer face. □

Analogously, we define a family of embedded series-parallel graphs $S(k)$. There are many ways of defining series-parallel graphs. One that will be convenient for us is that they are the graphs that can be reduced to a single edge by reduction operations that replace a path through a degree-two vertex by a single edge, and then if that produces multiple edges connecting the same two vertices, replacing those multiple edges by a single edge [4].

Definition 2 *We define $S(k)$ to be the embedded graph constructed as follows. Again, each such graph will have two yellow vertices and $2k$ blue vertices, connected in the pattern of a complete bipartite graph $K_{2,2k}$. For each yellow–blue edge e of this graph, we add a path of $2k-1$ red vertices. We connect every vertex in this path to the blue endpoint of e, and we connect one endpoint of the path to the yellow endpoint of e. Unlike $B(k)$ it is not true that $S(k)$ has a unique embedding; instead, we fix an embedding of $S(k)$ in which every yellow–blue quadrilateral contains either zero or four red paths, as shown in Fig. 2.*

The resulting graph has two yellow vertices, $2k$ blue vertices, and $4k(2k-1)$ red vertices, for a total of $8k^2-2k+2$ vertices. The yellow and blue vertices have degree $4k$, while the red vertices have
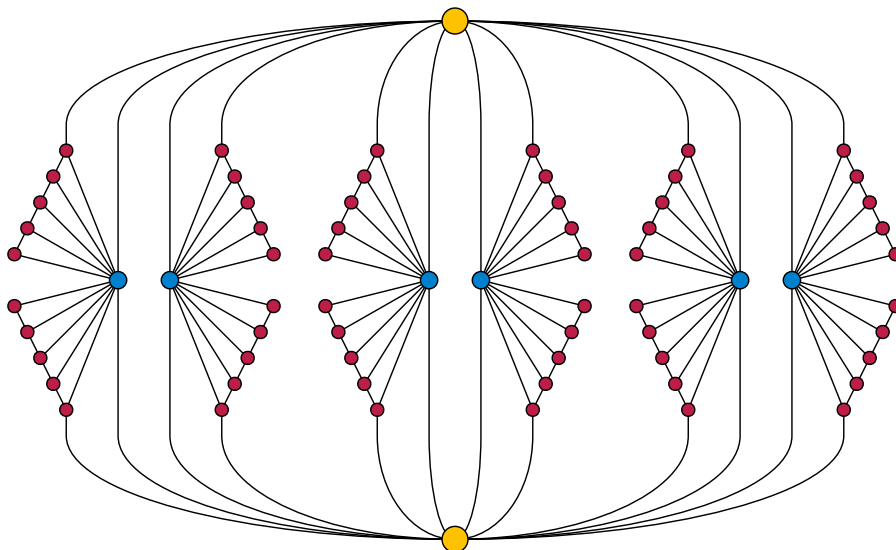
Figure 2: The embedded series-parallel graph $S(3)$ formed by our construction.

degrees two or three. The degree-two red vertices can be removed one at a time by series-parallel reduction operations, and after all red neighbors of a blue vertex have been removed in this way the blue vertex can also be removed by another series-parallel reduction operation, leaving only a single remaining edge between the two yellow vertices. Because these operations succeed in reducing $S(k)$ to a single edge, $S(k)$ is series-parallel.

We claim that, for sufficiently large values of k, the graph $G(k)$ and the embedded graph $S(k)$ do not have planar Lombardi drawings. Therefore, neither every planar bipartite graph nor every embedded series-parallel graph has a planar Lombardi drawing. In the remainder of this paper we prove this claim.

3   Equiangular arc-quadrilaterals

The key feature of both of our graph constructions $B(k)$ and $S(k)$ is the existence of many yellow–blue quadrilateral faces in which all vertices have equal and high degree; this degree is $2k$ in $B(k)$ and $4k$ in $S(k)$. If such a graph is to have a Lombardi drawing, each of these faces must necessarily be drawn as a quadrilateral with circular-arc sides and with the same interior angle ($2\pi/2k$ or $2\pi/4k$ respectively) at all four of its vertices. Equiangular arc-quadrilaterals have been investigated before from the point of view of conformal mapping [2]; in this section we investigate some of their additional properties.

We begin with a simple construction for these shapes, which we will later see is universal, in the sense that every equilateral arc-quadrilateral is the Möbius transform of one that is formed in the following way.

Lemma 2 *Let four circles in the plane be placed with their center points on a rhombus, with opposite circles in this cycle of four circles disjoint and having equal radii, and with consecutive*
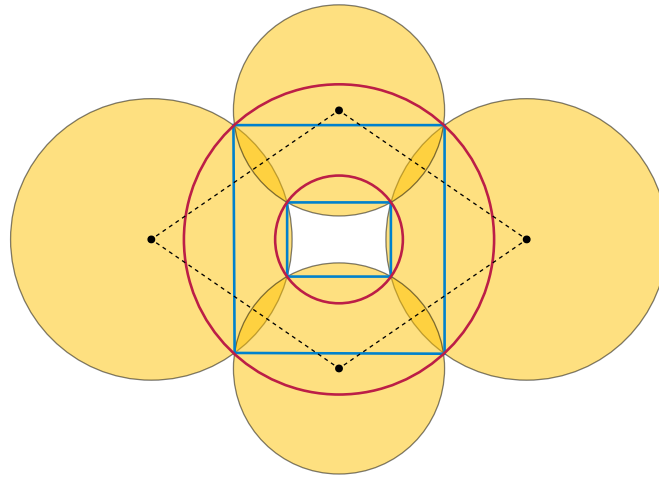
Figure 3: Illustration for Lemma 2: Four circles (yellow) with centers on a rhombus (dashed black), and with opposite pairs of circles having equal radii, have a union whose boundary consists of two equilateral arc-quadrilaterals with vertices on two rectangles (blue). The red circles contain the vertices of these arc-quadrilaterals according to Lemma 3.

circles in this cycle crossing each other, as shown in Fig. 3. Then the union of the four disks bounded by these circles is a topological annulus whose inner and outer boundaries form equiangular arc-quadrilaterals. Each of these arc-quadrilaterals has vertices that lie on a rectangle.

Proof: Each side of the rhombus is covered by the two disks centered on its endpoints, so the four disks entirely cover the rhombus boundary. However, they do not cover the center point of the rhombus because of the assumption that opposite circles are disjoint, so the center is part of an uncovered region entirely surrounded by covered regions, topologically an annulus. Its boundaries are formed by arcs of the circles, meeting at the crossing points, and again because opposite circles cannot meet these boundaries must be composed of four arcs.

The overall configuration of circles has the symmetries of a rhombus, with two perpendicular axes of reflection symmetry that each swap two of the circles and leave the other two circles unchanged. Because each crossing point belongs to one of the two swapped circles and one unchanged circle, these reflection symmetries swap the crossing points in pairs. Therefore, the convex hull of the four vertices of one of the boundary arc-polygons must be a rectangle, the only shape in the plane that has four points swapped in pairs by two perpendicular reflection symmetries.   □

The same construction with a cycle of four circles that are tangent in cyclically consecutive pairs, rather than crossing, can be seen as a degenerate limiting case, producing equiangular arc-quadrilaterals with vertex angle zero. As the next lemma shows, transforming to the configurations of Lemma 2 proves the existence of a circumscribing circle for every equilateral arc-quadrilateral:

Definition 3 *We say that an arc-quadrilateral is* cyclic *when its four vertices lie on a circle and the arcs of the quadrilateral are either all inside the circle or all outside the circle.*

Lemma 3 *Let abcd be a non-self-crossing quadrilateral in the plane with circular-arc sides and equal interior angles. Then abcd is cyclic.*

Proof: The properties of being an equiangular non-self-crossing circular-arc quadrilateral and of being cyclic are both invariant under Möbius transformations, which preserve both co-circularity of points and the crossings and crossing angles of curves. Therefore, if we can find a Möbius transformation of a given equiangular circular-arc quadrilateral such that the transformed quadrilateral is cyclic, the original quadrilateral will also be cyclic, as the lemma states it to be.

Start by finding a Möbius transformation which makes two opposite arcs ab and cd come from circles with the same radius as each other. An inversion through a unit circle centered at a point on one arc (a special case of a Möbius transformation) will cause the transformed image of that arc to have infinite radius while keeping the other radius finite, so if we continuously move the center of inversion from one arc to the other, by the intermediate value theorem, some point in this motion will be a center of inversion having the desired property. After this transformation, because of the equality of crossing angles, and by symmetry, both of the other two circular arcs bc and ad must come from circles whose centers lie on the line L midway between ab and cd. Because L separates ab from cd, but arcs bc and ad have their endpoints on the two separated arcs, L must be crossed by arcs bc and ad.

For each point p of L, there is a unique circle C_p centered at p that is perpendicular to the circles through arcs ab and (by symmetry) cd. Inverting through C_p leaves these two circles unchanged, but can nontrivially transform the other two circles and the arcs bc and ad contained in these other two circles. In particular, when p is the crossing point of L with bc, this transformation causes the transformed image of bc to have infinite radius while keeping the other radius finite. Symmetrically, when p is the crossing point of L with ad, inverting through C_p causes the transformed image of ad to have infinite radius while keeping the other radius finite. By continuously moving p from the crossing of L with bc to the crossing of L with ad, and again using the intermediate value theorem, we obtain a point p and an inversion through a circle C_p that leaves the circles through ab and cd fixed and that transforms the circles through bc and ad into two circles of equal radius.

For two circles of fixed size, the distance between their centers is a monotonic function of their crossing angle. Since, after the transformation, the four pairs of circles each have the same pair of sizes and the same crossing angles, their four distances between centers are equal, so the centers form the vertices of a rhombus with the circles centered at opposite vertices having the same radius as each other, meeting the conditions of Lemma 2. If the interior angle of $abcd$ is less than π, then the transformed copy of $abcd$ must lie within the circle that circumscribes the inner rectangle, forming the boundary of a hole in the union of the four transformed disks. If the interior angle is greater than π, it must lie outside the outer circle, forming the outer boundary of the union of the four disks. In either case, the transformed copy of $abcd$ is cyclic, so $abcd$ itself must be cyclic. □

A special case of Lemma 3 for right-angled arc-quadrilaterals was used previously by the author to prove that some 4-regular planar graphs have no planar Lombardi drawing [8]. Another special case, for arc-quadrilaterals in which all interior angles are zero, has been used previously in mesh generation [1].

The shape of an equiangular arc-quadrilateral, up to Möbius transformation, can be described by two real-number parameters, most simply by the vertex angles of the arc-quadrilateral and by the aspect ratio of the rectangles into which it can be transformed. However, for our purposes it is more convenient to replace the aspect ratio by a different parameter, which we define below in Definition 4 by reference to the circle of Lemma 3. Four *bigons* separate the arc-quadrilateral from this circle. As with any circular-arc bigon, the two interior angles in each bigons are equal, but different bigons may have different angles.
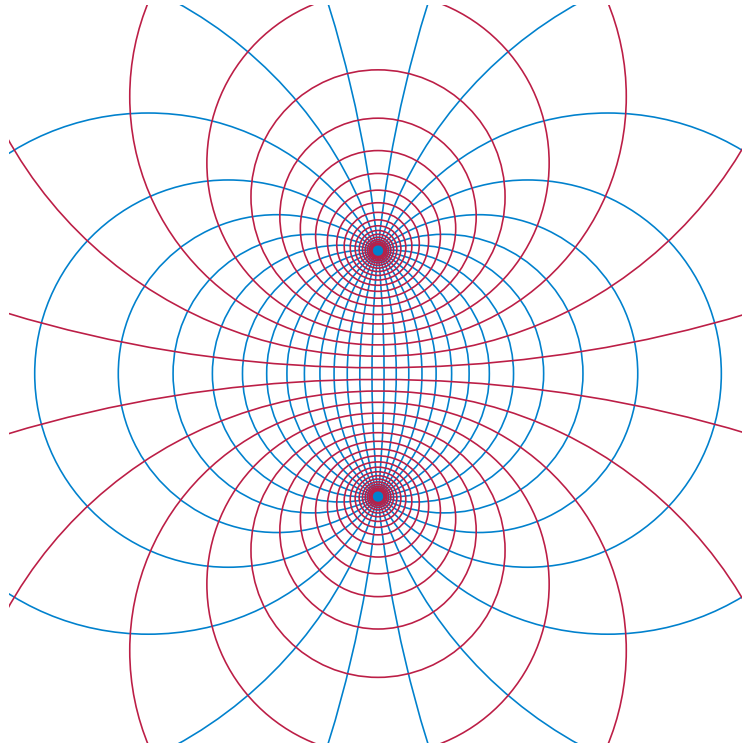
Figure 4: Curves of constant and evenly-spaced coordinate values for bipolar coordinates, forming two orthogonal pencils of circles.

Definition 4 *We define the* tilt *of an equiangular arc-quadrilateral to be the maximum interior angle of any of the four bigons separating the quadrilateral from its enclosing circle.*

Lemma 4 *Each vertex of an equiangular arc-quadrilateral is incident to a bigon whose interior angle is the tilt angle.*

Proof: Let Q be an equiangular arc-quadrilateral, and (by performing a Möbius transformation if necessary) assume without loss of generality that Q is enclosed by the circle C through its vertices. Let the interior angle of Q be θ, and let B be a bigon defining the tilt, with interior angle φ. Then at each of the two vertices of B, the other bigon incident to the vertex must have interior angle $\pi - \theta - \varphi$, in order to make the three angles of the bigons and quadrilateral at that vertex sum up to the total angle π spanned by the circle at that vertex. Repeating the same argument at the remaining two vertices shows that the bigon opposite B also has interior angle φ. Therefore, all four vertices are adjacent to a bigon with interior angle φ. $\qquad\square$

4   Bipolar coordinates

The *bipolar coordinate system* is a system of coordinates for points in the plane defined by reference to a pair of points s and t, which are called the *foci* of the coordinate system and which are not

assigned coordinates. The bipolar coordinates defined from these foci are conventionally denoted σ and τ.

Definition 5 *The σ-coordinate σ_p of a non-focus point p is the angle spt, which we will measure clockwise from ray ps to ray pt (so that, oriented in this way, angle tps would be the complement of angle spt). The τ-coordinate τ_p of p is the logarithm of the ratio of the two distances from p to the two foci.*

The level sets of the σ-coordinate are depicted as the blue circular arcs through the two foci in Fig. 4, and the level sets of the τ-coordinate are the red circles separating the two foci in the same figure. This coordinate system has the following convenient property that any (orientation-preserving) Möbius transformation that preserves the location of the two foci acts by translation on the coordinates, as formalized in the lemma below. This property can be seen as a reflection of the fact that the bipolar coordinate system comes from a conformal mapping of a rectangular grid [3].

Lemma 5 *For any Möbius transformation that preserves the location of the two foci, there exist θ and δ such that the transformation acts on bipolar coordinates of all points by adding θ to the σ-coordinate and δ to the τ-coordinate, where θ and δ depend only on the transformation and not on the location of the transformed point. That is, the transformation of a point with bipolar coordinates (σ, τ) is the point with bipolar coordinates $(\sigma + \theta, \tau + \delta)$.*

Proof: All Möbius transformations preserve circles, incidences between points and curves, and angles between pairs of incident curves. Therefore, any focus-preserving Möbius transformation takes circles through the two foci (the level sets for σ-coordinates) to other circles through the two foci, and it takes the perpendicular family of circles (the level sets for τ-coordinates) to other circles in the same family. Therefore it acts separately on the σ- and τ-coordinates.

Because the given Möbius transformation preserves both circles and angles, the images under the transformation of the level sets of the σ-coordinates (the blue arcs of Fig. 4) have the same relative angles as the level sets themselves. Because this relative angle determines the difference in σ-coordinates between pairs of level sets, it follows that the given transformation must act additively on the σ-coordinates.

To show that the transformation acts additively on τ-coordinate (the logarithm of the ratio of distances of a point from the two foci), we can assume without loss of generality (by scaling, translating, and rotating the plane if necessary) that the two foci are at the two points $q = \pm 1$ of the complex plane. Consider the general form $q \mapsto (aq + b)/(cq + d)$ of a Möbius transformation as a fractional linear transformation of the complex plane. For a transformation to fix $q = 1$ we need $a + b = c + d$ and for it to fix $q = -1$ we need $b - a = -(d - c)$. Solving these two equations in four unknowns gives $a = d$ and $b = c$. Therefore, the transformations fixing the foci take the special form $q \mapsto (aq + b)/(bq + a)$.

For a transformation of this form, and for any point x on the interval $[-1, 1]$ of real numbers with distance ratio $(1 + x)/(1 - x)$, the image of x has distance ratio

$$\frac{1 + (ax + b)/(bx + a)}{1 - (ax + b)/(bx + a)} = \frac{a + b}{a - b} \cdot \frac{1 + x}{1 - x},$$

multiplying the original distance ratio of x by a value that depends only on the transformation. Because the transformation acts separately on σ- and τ-coordinates, we obtain the same multiplicative action on distance ratios for any other point on the complex plane with the same τ-coordinate as x.
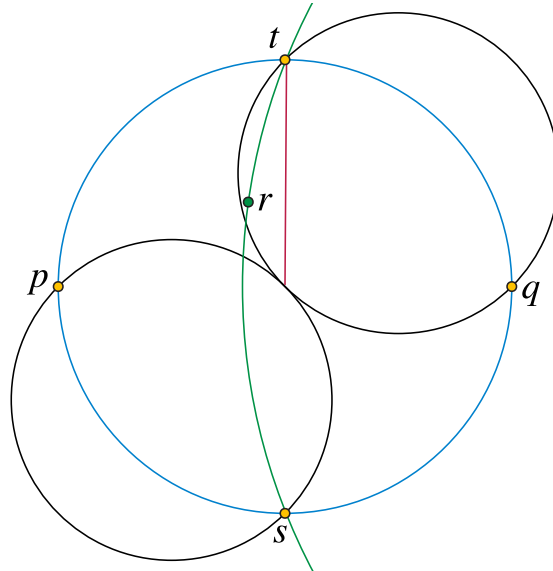
Figure 5: Illustration for Lemma 7: If quadrilateral *sptq* has high tilt, and *r* lies between the quadrilateral and its enclosing circle, to the left of the red arc, then *r* must have a higher τ-coordinate value than *p*. The illustration depicts an extreme case of the lemma, in which two bigons bounded by the black circles have tilt exactly $3\pi/4$ and are tangent to each other.

This multiplicative action on distance ratios translates into an additive action on their logarithms.
□

Beyond their additivity under Möbius transformations, another advantage of bipolar coordinates is that they provide a way of comparing angles at the two foci, that will be convenient for relating the tilts of different quadrilaterals to each other:

Lemma 6 *Let sptq be an equilateral arc-quadrilateral with interior angle θ and tilt φ, and suppose that the two bigons with angle τ (according to Lemma 4) are incident with s and p, and with t and q. Then, in the bipolar coordinate system with foci s and t, the difference between the limiting σ-coordinate of arc tp in the limit as it approaches t and of arc sq as it approaches s is exactly $2\theta + 2\varphi - \pi$.*

Proof: Let C be the circle through s, p, t, and q given by Lemma 3. Then arc tp meets C at t at the smaller of the angles of the two bigons, $\pi - \theta - \varphi$, so the σ-coordinate of the arc of C bounding this bigon can be obtained from the σ-coordinate of tp at t by subtracting this angle. In the same way, the σ-coordinate of sq at s can be obtained from the σ-coordinate of the same arc of C by adding the angles separating sq from that arc, which are φ for the digon separating sp from the arc, and θ for the angle of the arc-quadrilateral separating sp from sq. These additions and subtractions, going from the σ-coordinate of tp at t to the σ-coordinate of sq at s, have the stated total.   □

We can also use bipolar coordinates to show that heavily tilted quadrilaterals lead to an increase in τ-coordinate:

Lemma 7 *Let sptq be an equilateral arc-quadrilateral with tilt $\tau \geq 3\pi/4$, and suppose that the two bigons with angle τ (according to Lemma 4) are incident with s and p, and with t and q. Let r be a point in the bigon incident with t and q, such that circular arc srt makes an angle of at most $\pi/2$ with circular arc spt. Then, in the bipolar coordinate system for foci s and t, $\tau_r > \tau_p$.*

Proof: Let C be the circle through s, p, t, and q given by Lemma 3. Because of the Möbius invariance of coordinate differences in the bipolar coordinate system, we can without loss of generality and without changing the angles and coordinates of the lemma perform a Möbius transformation so that s, p, and t are the bottom, left, and topmost points of C. (This transformation will not necessarily place q as the rightmost point.) After this transformation, points above the horizontal line through p (which bisects st) will have higher τ-coordinate than o, and points below the horizontal line through o will have lower τ-coordinate.

Fig. 5 depicts an extreme case of the lemma, in which the tilt is exactly $3\pi/4$ and in which the two bigons with this tilt angle, incident to s and p and to t and q, are tangent to each other. The black circles of the figure bound these two bigons. For this choice of the tilt angle, the bigon through p and s passes through the center of the blue circle C through points s, p, t, and q. By symmetry, the opposite bigon through t and q is tangent to it at the center of C. By the assumption of the lemma, in this extreme case, r is inside the upper right circle, and (by the assumption on the angle of arc srt) is to the left of the red vertical line segment through the vertical diameter of circle C. Because all of the points that are to the left of the red line segment and inside the upper right circle are above the horizontal diameter of C, this must be true of r, showing that its τ-coordinate is greater than that of p.

In any other case of the lemma, possibly involving a greater value of the tilt, the lower left bigon can only be larger than or equal to the bigon depicted in the figure, causing the red segment to be shorter or equal. Regardless of its position, the upper right bigon makes a non-negative angle with C at t, and an equal angle at its lower crossing point with the red segment, so the red segment cuts from this bigon an arc that is at most a semicircle. Point r is confined to the region between this arc and the red segment; the bottom point of this region is on the red segment, and lies above the horizontal diameter of C, so again the τ-coordinate of r must be greater than that of p.   □

5   Nonplanarity

We are now ready for our main results.

Theorem 1 *Let G be an embedded planar graph that includes a set of $k \geq 8$ quadrilateral faces, all sharing two opposite vertices s and t, with all vertices of these faces having equal degrees. Suppose also that, at s and t, these faces are equally angularly spaced from each other. Then G does not have a planar Lombardi drawing.*

Proof: We will suppose that a planar Lombardi drawing exists and derive a contradiction from this assumption. We will consider a bipolar coordinate system with foci s and t, and label the vertices of each quadrilateral as sp_itq_i, with the neighbors of s appearing in the cyclic order $p_1, q_1, p_2, q_2, \ldots$. Because all vertices of these quadrilaterals have equal degrees, any planar Lombardi drawing must draw these quadrilaterals as equiangular arc-quadrilaterals, and by Lemma 3 each such quadrilateral is inscribed in a circle C_i and does not cross this circle.

Choose i such that the circles C_i and C_{i+1} meet each other at the sharpest angle formed by two circles that are consecutive in the cyclic order, and consider the pair of consecutive quadrilaterals
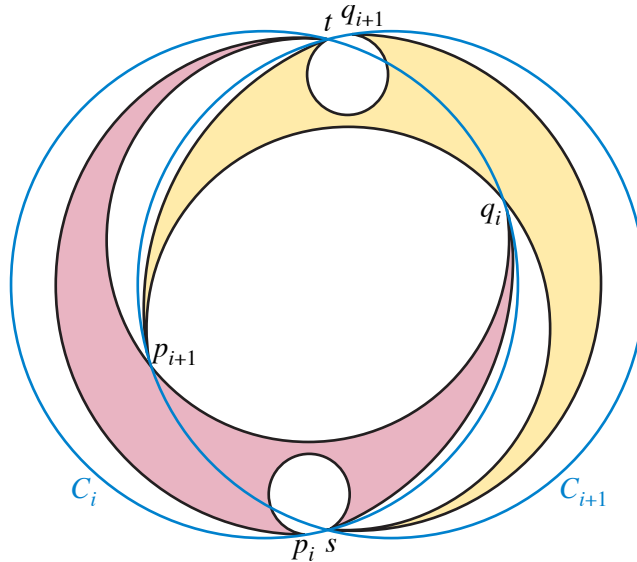
Figure 6: Two arc-quadrilaterals sp_itq_i and $sp_{i+1}tq_{i+1}$ with sharp angles between them at their shared vertices reach into each other's pockets to touch their circumscribing circles. The two smaller pockets on the outer arcs of the circles have significantly different τ-coordinates from each other in bipolar coordinates with the shared vertices as foci.

sp_itq_i and $sp_{i+1}tq_{i+1}$ circumscribed by these two circles. Fig. 6 shows one potential geometric realization for the circles C_i and C_{i+1} and their inscribed equiangular arc-quadrilaterals. By performing a Möbius transformation of the drawing, if necessary, we can assume that the two quadrilaterals are interior to their two circles, as shown in the figure, making it easier to describe the relative positions of the quadrilaterals and circles. However they are realized, the sum of the angles between the k cyclically-consecutive pairs of circles is 2π so the angle between circles C_i and C_{i+1} is at most $2\pi/k \leq \pi/4$. Point q_i must belong to circle C_i and be interior to circle C_{i+1}, as shown in the figure, belonging to an arc of circle C_i interior to C_{i+1} but exterior to quadrilateral $sp_{i+1}tq_{i+1}$. This arc of C_i containing q_i extends from a crossing point of C_i with quadrilateral $sp_{i+1}tq_{i+1}$, to either s or t; by swapping the roles of s and t if necessary, we can assume without loss of generality that it reaches the lower vertex s, as shown in Fig. 6. Then, within any small-enough neighborhood of s, quadrilateral $sp_{i+1}tq_{i+1}$ lies between circles C_i and C_{i+1}, so it must have tilt $\geq 3\pi/4$.

Lemma 6 allows the tilt of this quadrilateral, originally defined in terms of its angle with C_{i+1}, to instead be determined in terms of a difference in σ-coordinates at s and t in the chosen bipolar coordinate system. By the assumption of equal spacing at s and t, all of the k chosen quadrilateral faces have the same coordinate difference and (by Lemma 6) the same tilt, so they all meet the precondition of having high tilt of Lemma 7. For any chosen quadrilateral sp_itq_i, the point p_{i+1} of the next quadrilateral is connected to s by an arc of quadrilateral $sp_{i+1}tq_{i+1}$ that (again using the assumption of equal spacing) makes an angle of $2\pi/k$ with arc sp_i (Fig. 7, left). In order to apply Lemma 7 we need a small angle between C_i and C_{i+1} rather than a small angle between these two quadrilateral arcs, but (because of the high tilt) each circle makes an angle at s with the corresponding quadrilateral arc of at most $2\pi/k$ (Fig. 7, right). The angle between C_i and C_{i+1} can be at most the angle between the quadrilateral arcs, plus the angle between one of the two circles
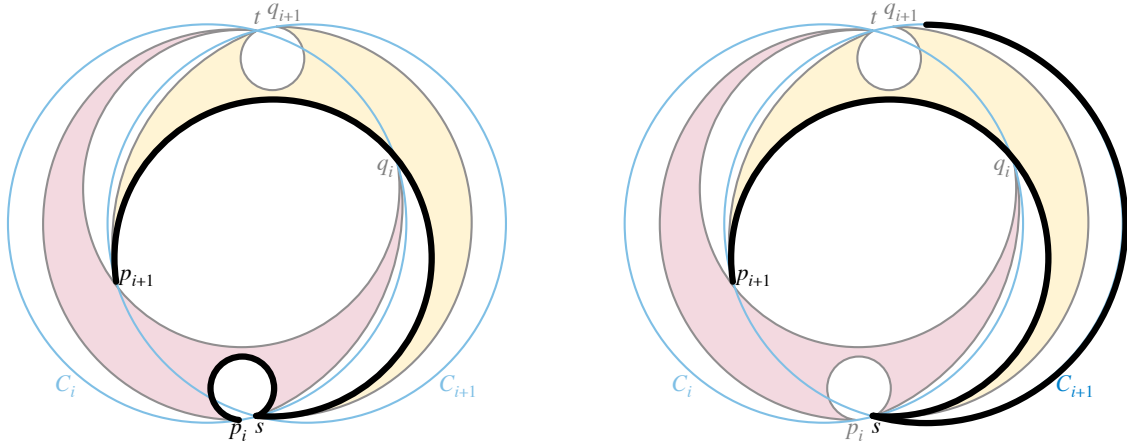
Figure 7: In the proof of Theorem 1, arcs sp_i and sp_{i+1} (left) make an angle of exactly $2\pi/k$ where they meet at point s, and arc sp_{i+1} makes an angle at s with the adjacent arc of circle C_{i+1} (right) of at most $2\pi/k$, so the arc of circle C_i between arcs sp_i and sp_{i+1} must make an angle of at most $4\pi/k$ with the arc of circle C_{i+1}.

and its quadrilateral arc, which is $4\pi/k \le \pi/2$. Thus, point p_{i+1} meets the other precondition of Lemma 7 for the position of the point r with respect to the quadrilateral.

By Lemma 7, each point p_{i+1} has a greater τ-coordinate than p_i. But it is impossible for this monotonic increase in τ-coordinates to continue all the way around the circle of quadrilaterals surrounding the two foci and back to the starting point. This impossibility shows that the drawing cannot exist.   □

Corollary 1 *For $k > 8$, the bipartite graph $B(k)$ does not have a planar Lombardi drawing.*

Proof: For these values of k, the yellow-blue quadrilateral faces of the unique embedding of $B(k)$ meet the conditions of Theorem 1.   □

Corollary 2 *For $k > 8$ the series-parallel graph $S(k)$, embedded as shown in Fig. 2, does not have a planar Lombardi drawing.*

Proof: For these values of k the yellow-blue quadrilateral faces of the fixed embedding of $S(k)$ meet the conditions of Theorem 1.   □

The construction of $S(k)$ can be adjusted in several different ways to obtain more constrained families of embedded series-parallel and related graphs that, again, have no planar Lombardi drawing:

Corollary 3 *There exists a family of embedded maximal series-parallel graphs (that is, embedded 2-trees) with no planar Lombardi drawing.*

Proof: Modify $S(k)$ by adding a two-edge path between the two yellow vertices in each yellow-red face, and then replace one of these paths by a single edge. Additionally, increase the length of the red chains so that the blue vertices of the modified graph continue to have the same degree as the yellow vertices. This modification produces an embedded maximal series-parallel graph in which the yellow-blue quadrilateral faces meet the conditions of Theorem 1.   □

Corollary 4 *There exists a a family of embedded bipartite series-parallel graphs with no planar Lombardi drawing.*

Proof: Modify $S(k)$ by replacing each yellow–red and red–red edge by a two-edge paths. The modification does not affect the degree or even spacing of the yellow-blue quadrilateral faces, which continue to meet the conditions of Theorem 1. □

Corollary 5 *There exists an embedded apex-tree (a graph obtained by adding a single vertex to a tree) with no planar Lombardi drawing,*

Proof: Modify $S(k)$ by deleting all red-red and yellow-red edges, and reducing the number of red vertices so that the blue vertices continue to have equal degree to the yellow vertices. The resulting graph is an apex-tree (with either of the two yellow vertices as its apex) and its yellow-blue quadrilateral faces continue to meet the conditions of Theorem 1. □

6   Conclusions

We have shown that bipartite planar graphs, and series-parallel graphs with a fixed planar embedding, do not always have planar Lombardi drawings, even though their low degeneracy implies that they always have (nonplanar) Lombardi drawings. In the conference version of this paper, we asked about planar Lombardi drawings of another kind of planar graph, the cactus graphs; subsequently, we have shown that these always have planar Lombardi drawings for their natural embeddings, but not for certain other embeddings [9].

In the question of which important subfamilies of planar graphs have planar Lombardi drawings, several important cases remain unsolved. These include the outerplanar graphs, both with and without assuming an outerplanar embedding and the series-parallel graphs without a fixed choice of embedding. We leave these as open for future research.

References

[1] M. Bern, S. Mitchell, and J. Ruppert. Linear-size nonobtuse triangulation of polygons. *Discrete & Computational Geometry*, 14(4):411–428, 1995. `doi:10.1007/BF02570715`.

[2] P. R. Brown and R. M. Porter. Conformal mapping of circular quadrilaterals and Weierstrass elliptic functions. *Computational Methods and Function Theory*, 11(2):463–486, 2011. `doi:10.1007/BF03321872`.

[3] J.-T. Chen, M.-H. Tsai, and C.-S. Liu. Conformal mapping and bipolar coordinate for eccentric Laplace problems. *Computer Applications in Engineering Education*, 17(3):314–322, 2009. `doi:10.1002/cae.20208`.

[4] R. J. Duffin. Topology of series-parallel networks. *Journal of Mathematical Analysis and Applications*, 10:303–318, 1965. `doi:10.1016/0022-247X(65)90125-3`.

[5] C. A. Duncan, D. Eppstein, M. T. Goodrich, S. G. Kobourov, M. Löffler, and M. Nöllenburg. Planar and poly-arc Lombardi drawings. *Journal of Computational Geometry*, 9(1):328–355, 2018. `doi:10.20382/jocg.v9i1a11`.

[6] C. A. Duncan, D. Eppstein, M. T. Goodrich, S. G. Kobourov, and M. Nöllenburg. Lombardi drawings of graphs. *J. Graph Algorithms & Applications*, 16(1):85–108, 2012. `doi:10.7155/jgaa.00251`.

[7] C. A. Duncan, D. Eppstein, M. T. Goodrich, S. G. Kobourov, and M. Nöllenburg. Drawing trees with perfect angular resolution and polynomial area. *Discrete & Computational Geometry*, 49(2):157–182, 2013. `doi:10.1007/s00454-012-9472-y`.

[8] D. Eppstein. A Möbius-invariant power diagram and its applications to soap bubbles and planar Lombardi drawing. *Discrete & Computational Geometry*, 52(3):515–550, 2014. `doi:10.1007/s00454-014-9627-0`.

[9] D. Eppstein, D. Frishberg, and M. C. Osegueda. Angles of arc-polygons and Lombardi drawings of cacti. In *Proc. 33rd Canadian Conference on Computational Geometry*, pages 56–64, 2021. `arXiv:2107.03615`.

[10] P. Kindermann, S. Kobourov, M. Löffler, M. Nöllenburg, A. Schulz, and B. Vogtenhuber. Lombardi drawings of knots and links. *Journal of Computational Geometry*, 10(1):444–476, 2019. `doi:10.20382/jocg.v10i1a15`.